Briefing Space Weather

2023/06/07

1 Sun

1.1 Responsible: José Cecatto

05/29 – No (M/X) flare; Fast wind stream (=< 450 km/s); 11 CME c.h.c. toward the Earth;
05/30 – M1.2, M1.3, M1.4 flares; No fast wind stream; 8 CME c.h.c. toward the Earth;
06/31 – M1.3, M1.0, M4.2 flares; No fast wind stream; 9 CME c.h.c. toward the Earth;
06/01 – No (M/X) flare; Fast wind stream (=< 500 km/s); 5 CME c.h.c. toward the Earth;
06/02 – M1.5 flare; No fast wind stream; 3 CME c.h.c. toward the Earth;
06/03 – No (M/X) flare; No fast wind stream; 7 CME c.h.c. toward the Earth;
06/04 – No (M/X) flare; No fast wind stream; 6 CME c.h.c. toward the Earth;
06/05 – No (M/X) flare; Fast wind stream (=< 450 km/s); 3 CME c.h.c. toward the Earth
Prev.: Fast wind stream for the next 02-04 days; for the next 2 days (35% M, 10% X) probability of M / X flares; also,
occasionally other CME can present component toward the Earth.
c.h.c. – can have a component; * partial halo; ** halo

2 Sun

2.1 Responsible: Douglas Silva

- WSA-ENLIL (CME 2023-05-29T02:12 UT)
  - The simulation results indicate that the flank of CME will reach the DSCOVR mission between 2023-06-01T10:00 UT and 2023-06-02T00:00 UT.
- WSA-ENLIL (CME 2023-05-30T17:12 UT)
  - The simulation results indicate that the flank of CME will reach the DSCOVR mission between 2023-06-04T00:00 UT and 2023-06-04T14:00 UT.
- WSA-ENLIL (CME 2023-06-04T10:24 UT)
  - The simulation results indicate that the CME will reach the DSCOVR mission between 2023-06-07T06:14 UT and 2023-06-07T20:14 UT.

Coronal holes (SPOCA):

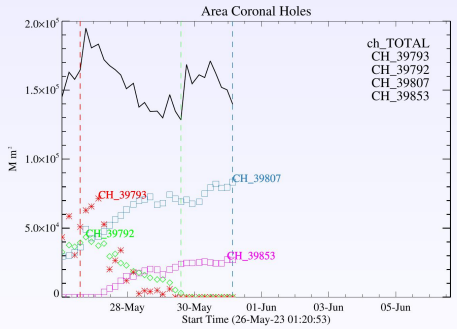

Figura: The solid black line depicts the products of the sum of areas for each detection interval performed by SPOCA between May 26 and 31, 2023.

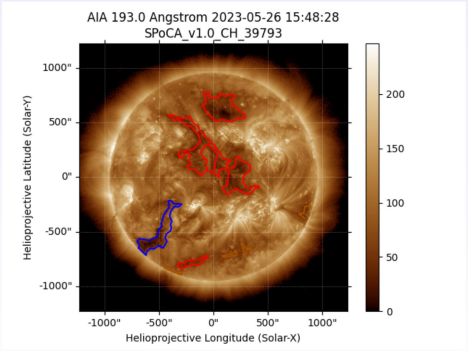

Figura: Above the 193 Å image of the Sun are highlighted coronal holes observed by SPOCA around 15:40 UT on May 26, 2023 (red dot line).

Coronal holes (SPOCA):

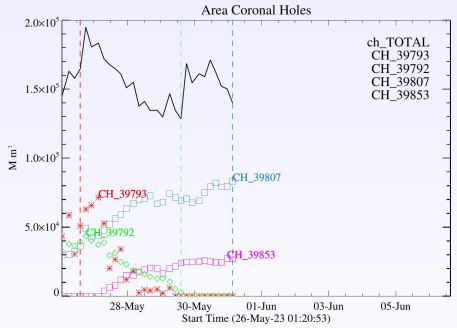

Figura: The solid black line depicts the products of the sum of areas for each detection interval performed by SPOCA between May 26 and 31, 2023.

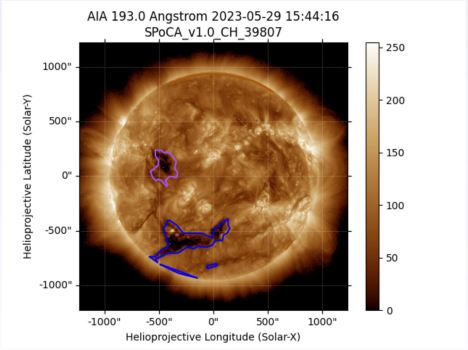

Figura: Above the 193 Å image of the Sun are highlighted coronal holes observed by SPOCA around 15:40 UT on May 29, 2023 (green dot line).

Coronal holes (SPOCA):

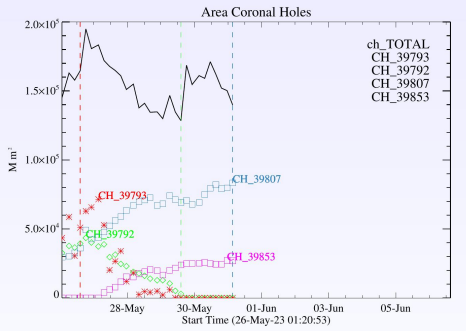

Figura: The solid black line depicts the products of the sum of areas for each detection interval performed by SPOCA between May 26 and 31, 2023.

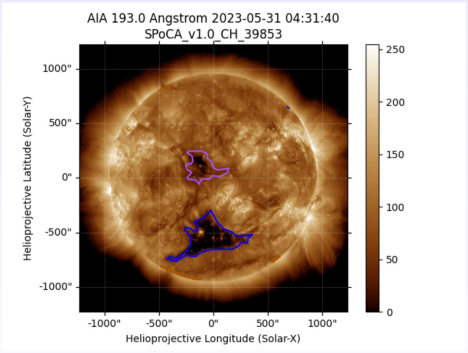

Figura: Above the 193 Å image of the Sun are highlighted coronal holes observed by SPOCA around 04:30 UT on May 31, 2023 (blue dot line).

WSA - ENLIL and SPOCA

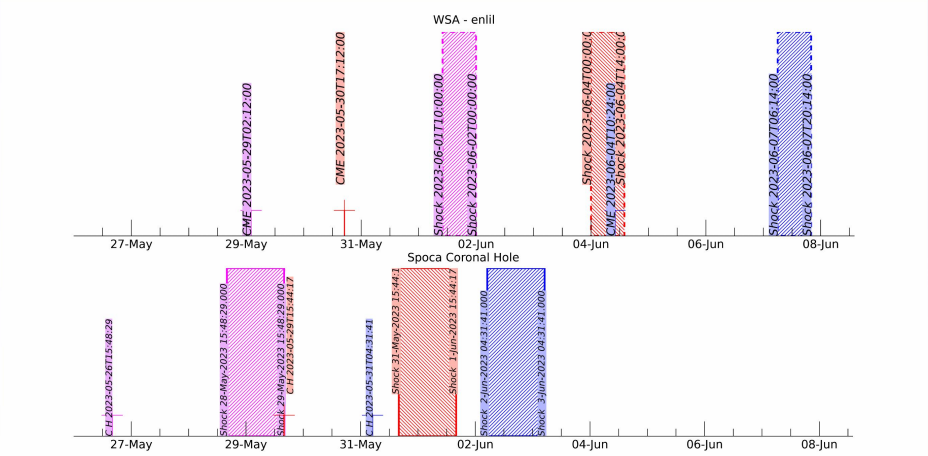

3 Interplanetary medium

3.1 Responsible: Paulo Jauer

- The modulus of the interplanetary magnetic field component showed a maximum peak of 31 nT on Apr/24 at 01:30 UT during the analyzed period.
- Two peaks of 16 nT and 17 nT were also detected on April 6 and 7 at 04:30 and 15:30 UT respectively.
- The BxBy components presented variations in the analyzed period, keeping both oscillating within the interval [+15, -30] nT, without the presence of sector change. The IMF By component showed a minimum value of -30 nT on Apr/24 at 10:30 UT.
- The component of the bz field showed a minimum value on 24/Apr at 02:30 UT of -29 nT. During the interaction of the CME-type structure that interacted with the global and inner magnetosphere. The Bz component also showed a minimum value on May 06 at 03:30 UT of -13 nT.
- The solar wind density showed peaks on 23/Apr 06/May and 07/May at 19:30, 03:30 and 14:50 UT of 27, 30 and 29 p/cm^3 due to interplanetary structure interaction.

- The solar wind speed remained on average above 400 km/s with a peak on 28/Apr at 16:30 UT of 691 km/s.
- The position of the magnetopause was oscillating with a minimum value recorded on 23/Apr at 19:30 UT of 5.9 Re and on 06/May at 03:30 UT of 6.8 Re. On average, the position of the magnetopause was above the equilibrium position.

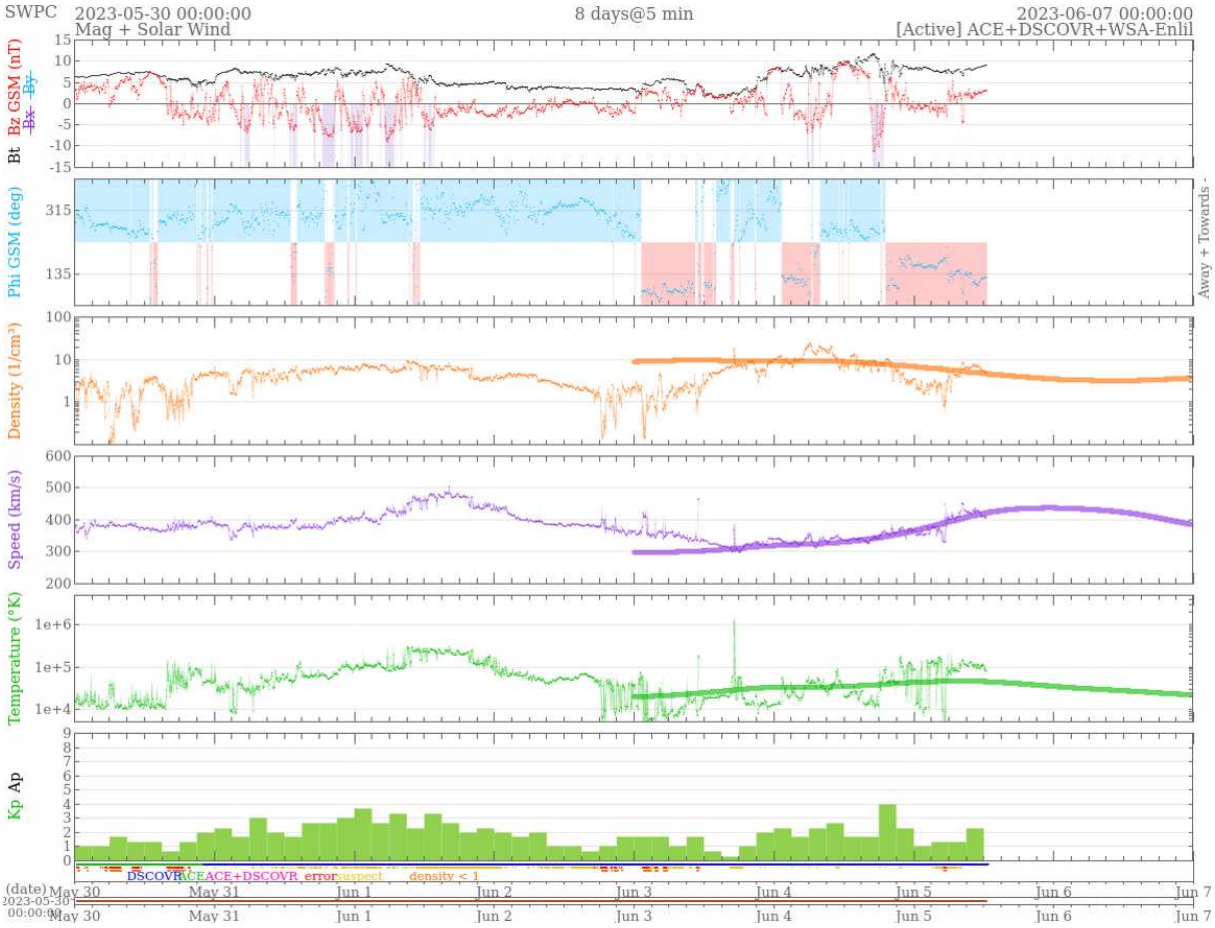

4 Radiation Belts

4.1 Responsible: Ligia Alves da Silva

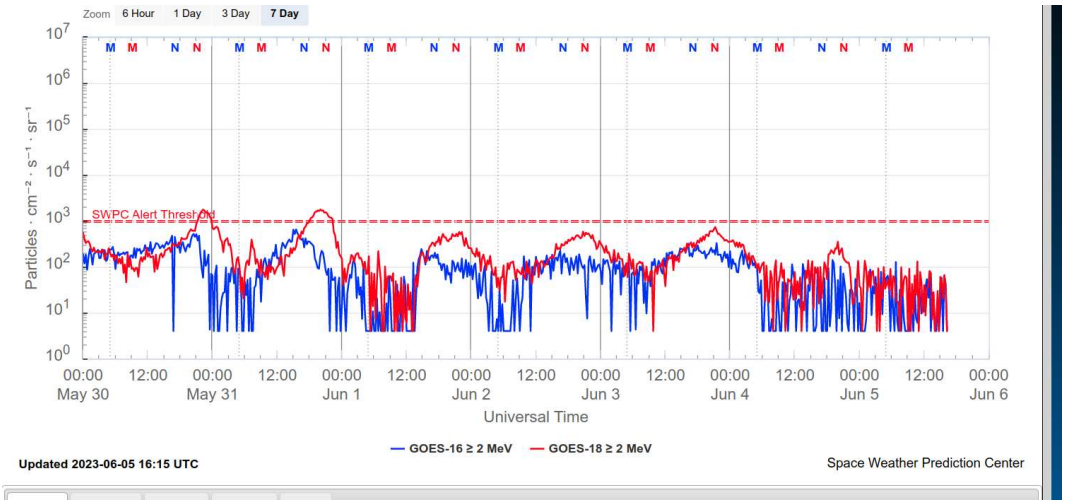

Figura 1: High-energy electron flux (> 2MeV) obtained from GOES-16 and GOES-18 satellite. Source:`https://www.swpc.noaa.gov/products/goes-electron-flux`.

High-energy electron flux (> 2 MeV) in the outer boundary of the outer radiation belt obtained from geostationary satellite data GOES-16 and GOES-18 (Figure above) shows two peaks that exceed 103 particles/(cm2 sr) on June 30th and 31st, respectively. A first "dropout" is observed from 00:00 UT on June 1st, and a second from June 4th. The latter contributes to the confinement of the electron flux to be below 10^2 particles/$(cm^2 sr)$ for more than 24 hours.

5 ULF waves

5.1 Responsible: Graziela B. D. Silva

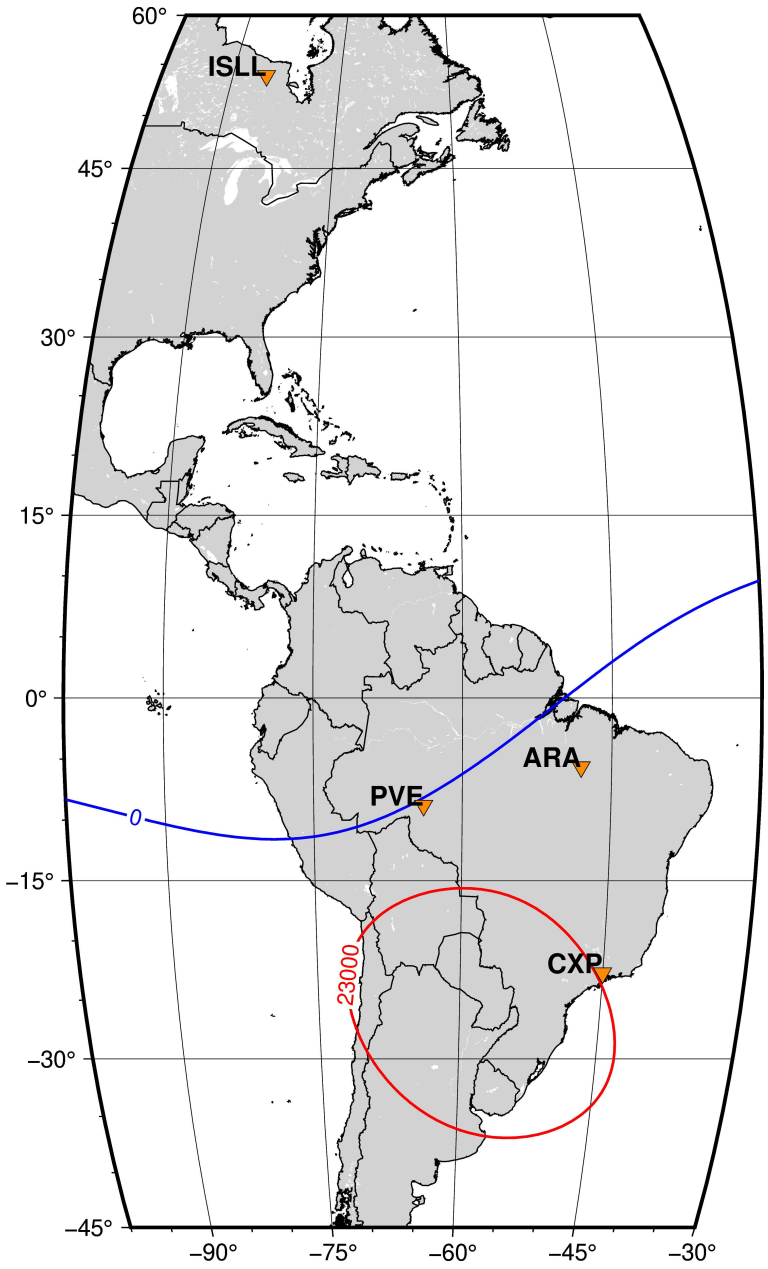

Figura 2: a) Map describing the geographic location of the stations together with the magnetic isolines to show that magnetic equator (blue) and the SAMA region (red). Cortesy: Karen Sarmiento.

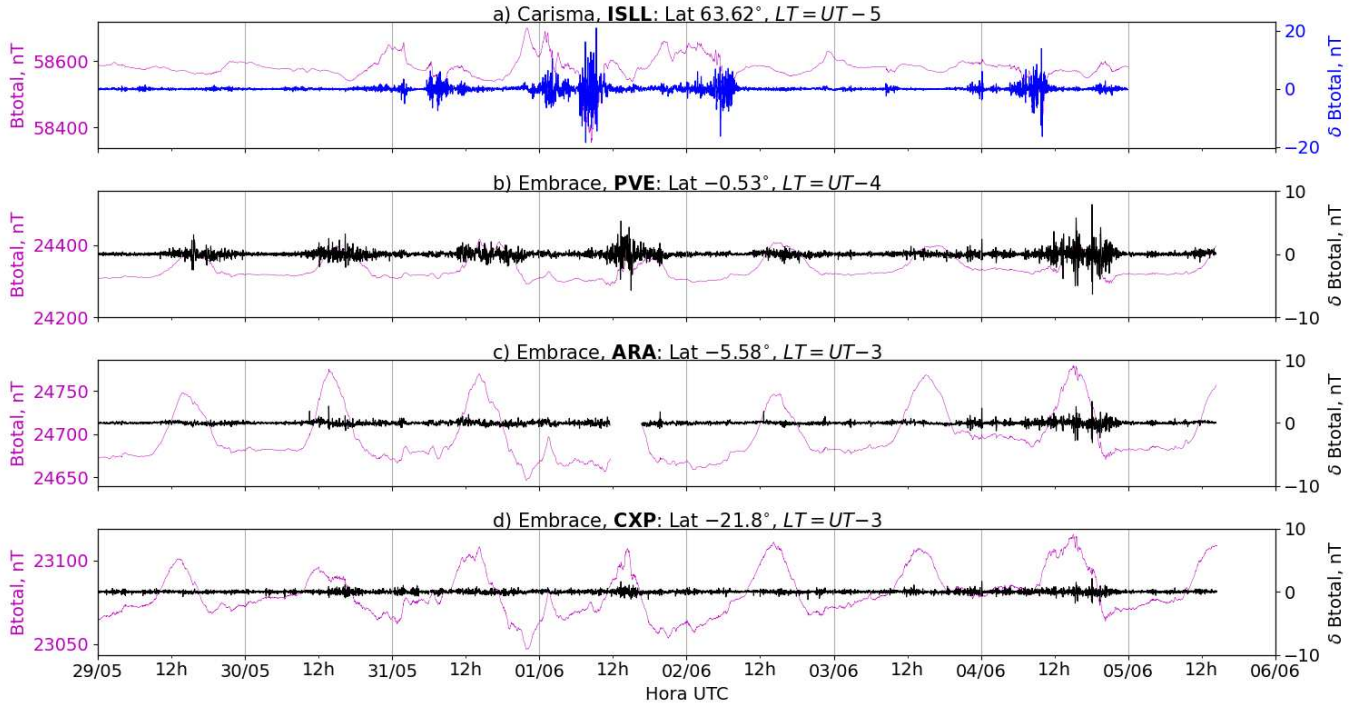

Figura 3: a) Timeseries of the geomagnetic field total component measured at ISLL station (Island Lake) of the CARISMA magnetometer network in magenta, along with the associated perturbation in the Pc5 band shown in blue. b-d) timeseries of the geomagnetic field total component measured at stations PVE (Porto Velho), ARA (Araguatins), and CXP (Cachoeira Paulista) of the EMBRACE network in magenta, along with the Pc5 perturbation in blue.

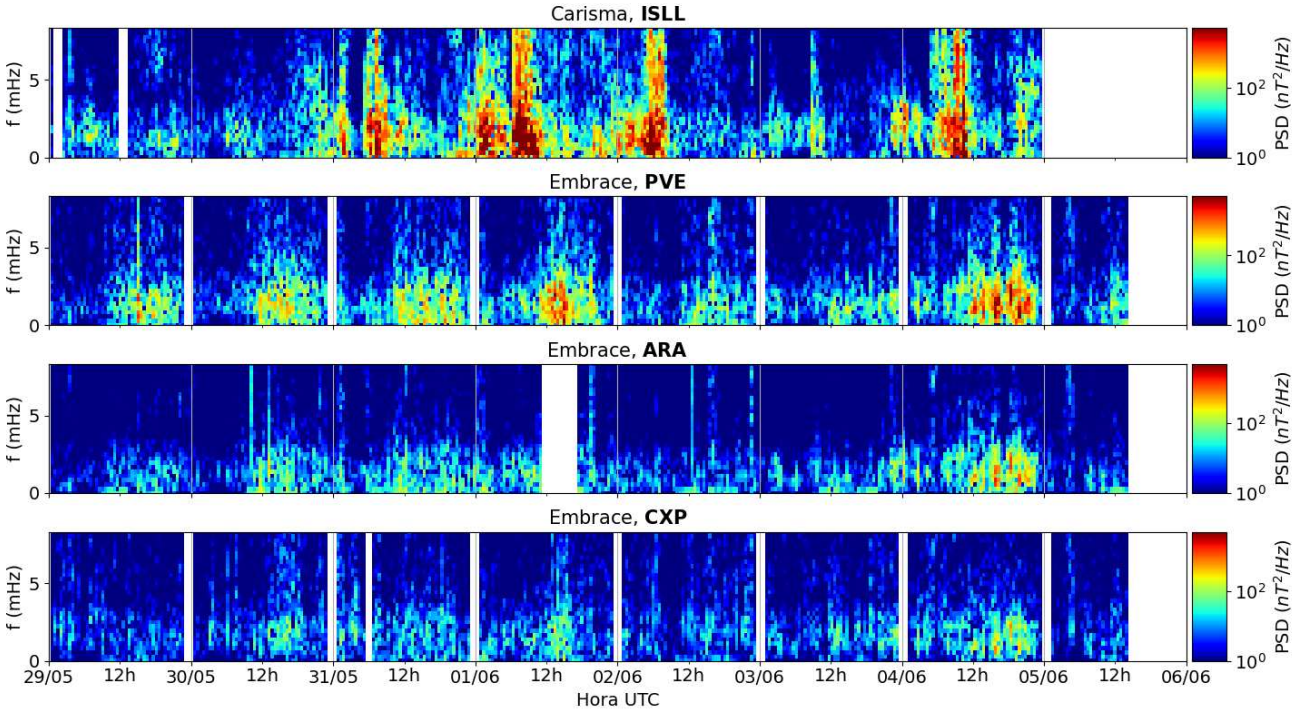

Figura 4: a-d) Time evolution of the power spectral density obtained from the filtered timeseries of the geomagnetic field total component (δ Btotal) for a) the high latitude station (ISLL-CARISMA), and b-d) for the low latitude stations of EMBRACE (PVE, ARA, CXP).

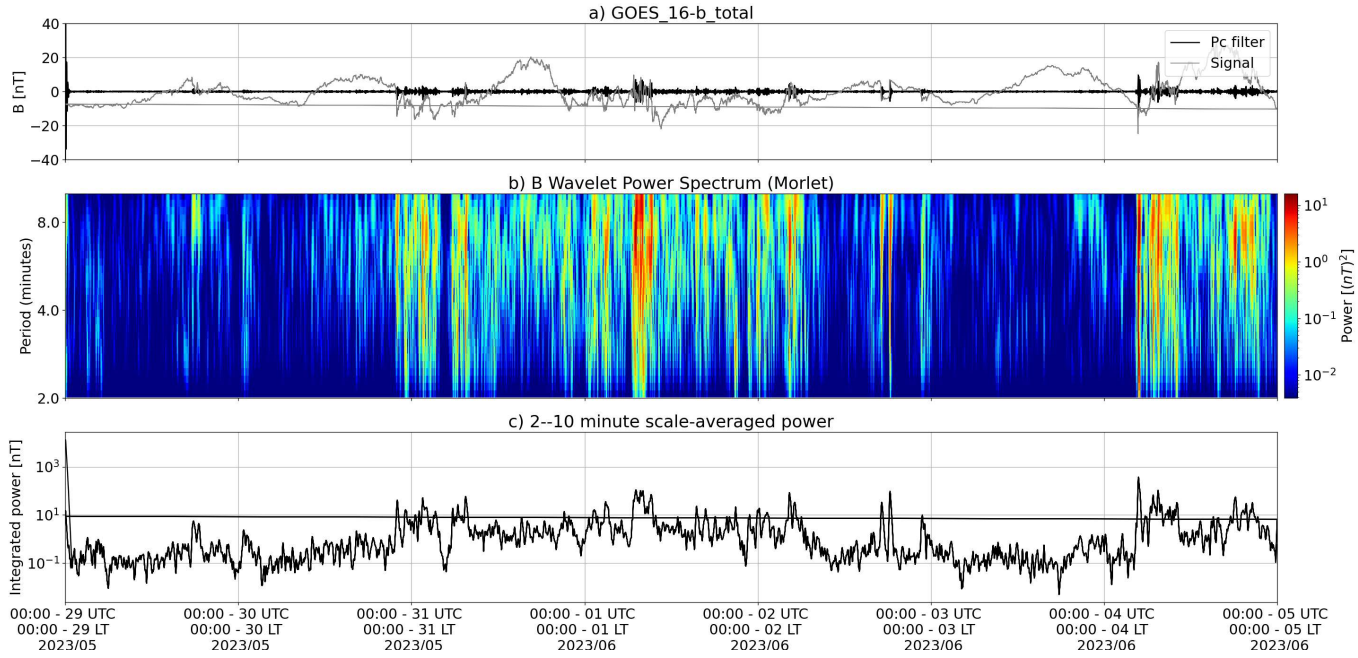

Figura 5: a) Timeseries of the geomagnetic field total component measured by GOES 16, together with the Pc5 fluctuation in black. b) Wavelet power spectrum of the filtered timeseries. c) Average ULF power in the period range from 2 to 10 minutes.

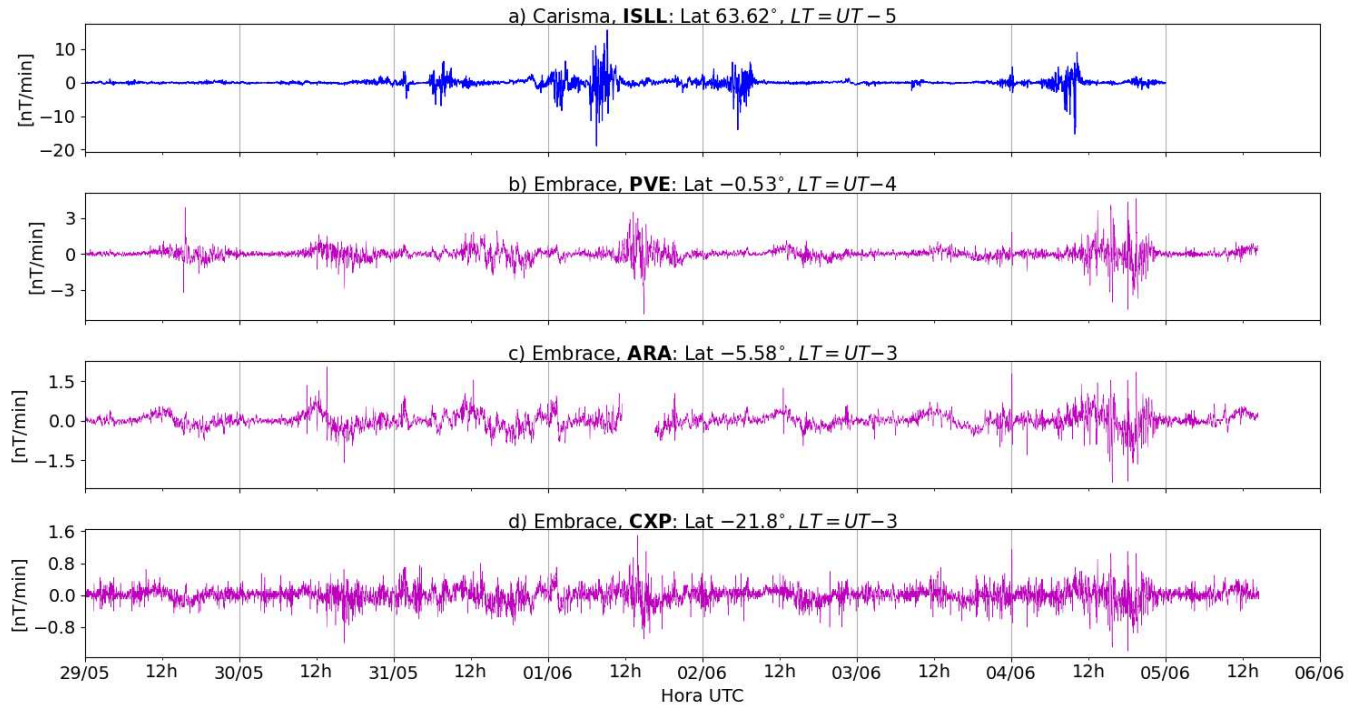

Figura 6: a-d) The rate of change of the geomagnetic field total component (dB/dt) obtained for a) the high latitude station (ISLL-CARISMA), and b-d) for the low latitude stations of EMBRACE (PVE, ARA, CXP).

- The GOES 16 satellite in geosynchronous orbit (L $\sim$ 6.6) registered significant activity of Pc5 ULF waves on May 31, and June 01, 02 and 04.
- As observed on the ground, the ISLL station at high latitude registered significant ULF wave

activity over the week.

- The PVE station from Embrace MagNet, located under the dip equator, registered moderate to intense activity of the waves activity during the week.
- The CXP and ARA stations at low latitudes of Brazil rather registered low activity of the waves over the week, excpet on June 04 due to arrival of an ICME.
- The dB/dt rates were below 20 nT/min in magnitude at ISLL (high latitude) and below 5 nT/min at the Embrace stations, with PVE exhibiting the highest values.
- There was detection of significant events of SI (sudden impulses or SCs with dB/dt¿5nT/min) over the week.

6 Geomagnetic activity

6.1 Responsible: Lívia Alves

From May 30 to June 05, the following events related to geomagnetic activity stand out:

- May 31 and Jun 01: geomagnetic field show to be unsettled.
- jun/01: H-component reached a minimum at 15 UT in PVE.
- The AE index surpassed 500 nT in May 31. The Dst index reached -31 nT (May 31) . The highest Kp of the week was 3o.

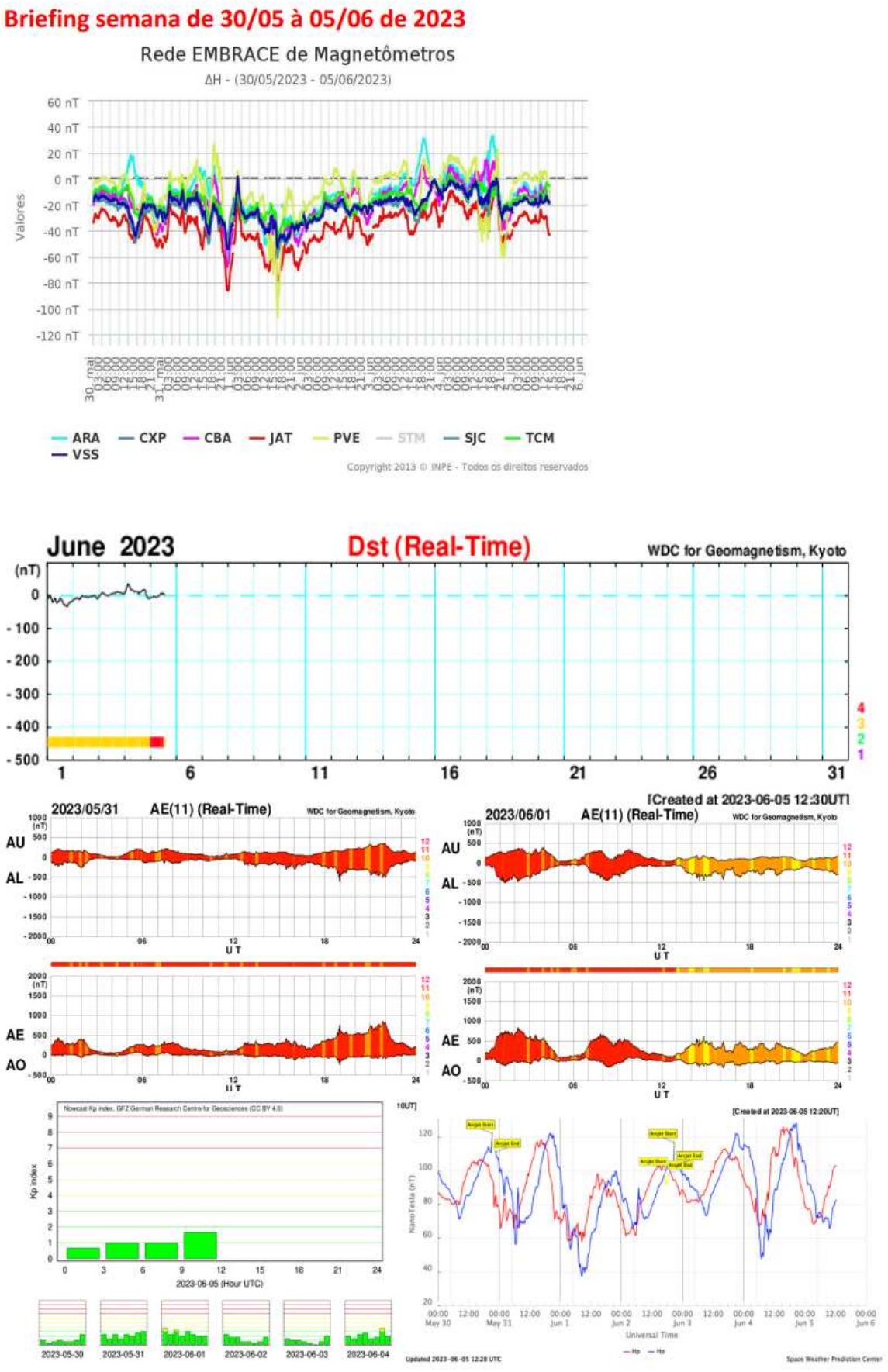

Figura 7: Time evolution of the geomagnetic field data and indices during the reported week.

7 ROTI

7.1 Responsible: Carolina de Sousa do Carmo

In the week 2264 (May 28 to June 03, 2023) there were no ionospheric irregularities (plasma bubble), on all analyzed days. Figure below shows the ROTI time series for four stations in the Brazilian sector (Natal (RNNA), Bacabal (MABB), Cuiabá (CUIB) and São José dos Campos (SJSP)).

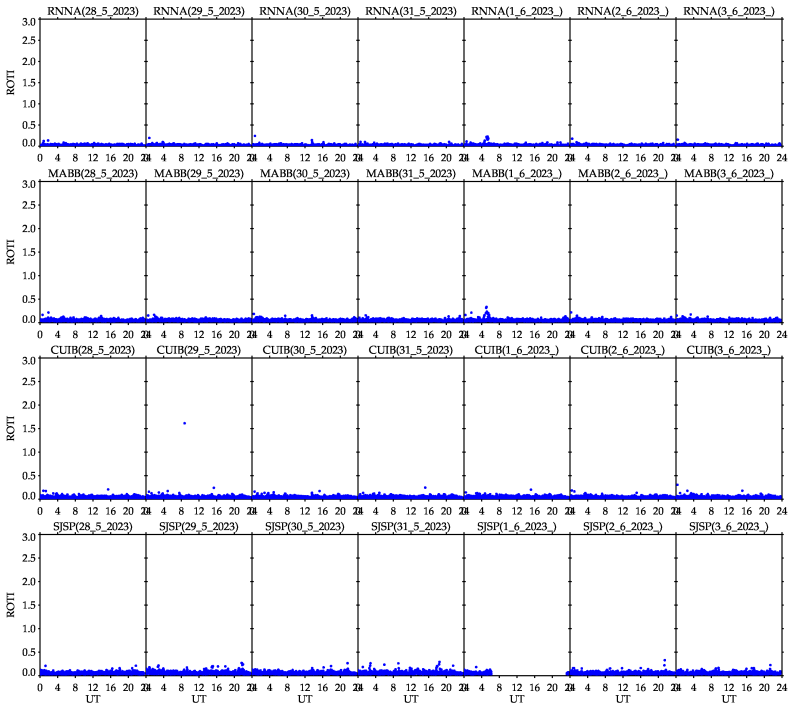

Figura 8: ROTI time series for four stations in the Brazilian sector (Natal (RNNA), Bacabal (MABB), Cuiabá (CUIB) and São José dos Campos (SJSP)), from May 28 to June 03, 2023.